Measurement of the Higgs quartic coupling c_2v from di-Higgs Vector Boson Fusion in the $b\bar{b}\tau^+\tau^-$ channel

Christos Paraskevopoulos
National Technical University of Athens, Heroon Polytechniou 9, Zografou, Greece
E-mail: christos.paraskevopoulos@cern.ch

Abstract. The Brout Englert Higgs (BEH) mechanism of electroweak symmetry breaking and mass generation was experimentally confirmed after the discovery of the Higgs boson at the Large Hadron Collider in 2012. The BEH mechanism not only predicts the existence of a massive scalar particle, but also requires this scalar particle to couple to itself. Double Higgs production provides a unique handle, since it allows the extraction of the trilinear Higgs self-coupling. VBF di-Higgs production also probes the quartic Higgs bosons to vector bosons coupling (c_2v). In this topic the effort on setting constraints on c_2v will be discussed. Event selection and reconstruction will be illustrated as well as a Neural Network designed to identify VBF events.

1. Introduction

The Higgs boson was discovered by the ATLAS and CMS collaborations in 2012 at the Large Hadron Collider [1] [2] . While the Brout-Englert-Higgs(BEH) mechanism predicts the existence of a massive scalar particle, the measurement of the Higgs boson trilinear self-coupling is a crucial validation of the BEH mechanism [3][4] [5][6]. In the Standard Model (SM) pairs of Higgs bosons are mainly produced via gluon-gluon fusion processes via a loop of top quarks and the Higgs self-interaction [7].

In the SM the BEH self coupling λ is uniquely determined by the structure of the scalar potential and is proportional to the product of the heavy-quark Yukawa coupling and the Higgs-boson self-coupling. However the existence of destructive interference between the box and the triangle diagram means di-Higgs production cross section has a small rate of $\sigma_{HH,SM} = 33fb$ at $\sqrt{s} = 13TeV$, about 1000 times smaller than single Higgs production [8]. In addition to constraining λ, in the vector-boson fusion (VBF) channel double Higgs production also probes the strength of the Higgs non-linear interactions with vector bosons at high energies and will allow us to set limits on Higgs quartic coupling c_2v [9]. Moreover, a variety of new physics models predict enhancements to this cross-section [10][11][12]. An example with a new heavy resonance is depicted in Fig.1.

Modifications of the Higgs top-quark Yukawa coupling or modifications of the Higgs self-coupling, or presence of new diagrams with new couplings could enhance the non-resonant di-Higgs production cross section [13] (see Fig.2). The SM HH production is not expected to be observed with the data so far collected by the ATLAS experiment. Beyond Standard Model (BSM) effects could enhance this rate [14]. Therefore, a search for Higgs pair production with current data is a probe of new physics.

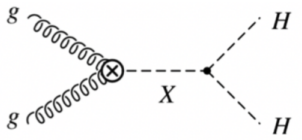

Figure 1. Theories beyond the SM (BSM) predict heavy resonances that could decay into a pair of the SM Higgs bosons, such as a heavy spin-0 scalar X in two-Higgs-doublet models (2HDM).The presence of such resonances would also enhance the di-Higgs production cross section.

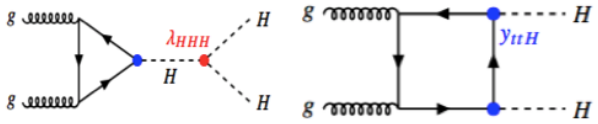

Figure 2. Leading-order Feynman diagrams for the gluon gluon fusion (ggF) non-resonant production of Higgs boson pairs: the "triangle diagram" and the "box diagram". The Higgs boson trilinear self-coupling is denoted λ_{HHH}. The Yukawa coupling of the Higgs to the top-quark is denoted by y_{ttH}

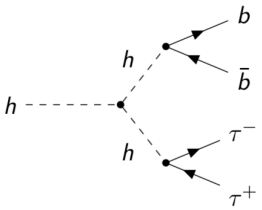

Figure 3. Depiction of the final state of $HH->bb\tau\tau$

The channel we are going to explore is the final state of $b\bar{b}\tau^+\tau^-$, see for example Fig.3. This state is the most sensitive channel with $36fb^{-1}$ data [15]. It represents a relatively clean final state compared to the channels with larger branching fractions ($b\bar{b}b\bar{b}$ and $b\bar{b}W^+W^-$) due to a better separation from the multijet and $\tau\tau$ backgrounds [16][17]. The $b\bar{b}\tau^+\tau^-$ channel has the third largest branching fraction (7.4%) of the experimentally feasible channels [18]. In the final state one of the two τ-leptons of the pair is required to decay hadronically, while the other decays either hadronically ($\tau_{had}\tau_{had}$) or leptonically ($\tau_{lep}\tau_{had}$). While the relatively small background and high branching ratio is an advantage of both decay channels, the *lephad* has a higher trigger efficiency (due to the lepton) while the *hadhad* higher purity (much less $\tau\tau$ background). In this paper we will focus on the *hadhad* channel.

2. What can we access with HH

The main categories we are going to focus are gluon gluon fusion (ggf), see Fig.2 and Vector Boson Fusion (VBF), see Fig.4. The SM predicts non-resonant HH production, with approximately 90% of the total cross-section being due to the ggf process [19].

This channel has been extensively studied in the literature and several final states have been considered, including $b\bar{b}\gamma\gamma$, $b\bar{b}\tau^+\tau^-$, $b\bar{b}W^+W^-$ and $b\bar{b}b\bar{b}$ (for a list of feasibility studies, see for example [20][21][22] [23][24][25]

Working in the infinite top mass approximation, the gluon-fusion di-Higgs production cross

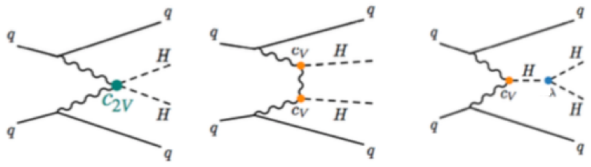

Figure 4. Possible BSM enhancements due to modified coupling strength of c_2v

section was calculated at NLO in [26] and NNLO in [27]. The resummation of soft-gluon emissions was performed at NNLL [28][29]. Recent studies indicate that Higgs pair production in gluon-fusion at the HL-LHC will allow the extraction of the Higgs self-coupling λ with accuracy.

Higgs pairs can also be produced in the VBF channel [9][30][31][32][33] where a soft emission of two vector bosons from the incoming protons is followed by the hard $VV->hh$ scattering, with $V = W, Z$. In the SM, the VBF inclusive cross section at 14 TeV is around 2 fb^{-1} which is more than one order of magnitude smaller than in gluon fusion [9].

Despite its small rate, Higgs pair production via VBF is quite interesting since even small modifications of the SM couplings can induce a striking increase of the cross section as a function of the di-Higgs mass [34].

In the following equation, the parameterization of the effective non-flavor-violating Higgs Lagrangian, in the case the couplings of the Higgs boson to the SM fermions scale with their masses, is given. There is also another parameter, c3, which is not shown:

$$\begin{aligned}\mathscr{L} \supset \frac{1}{2}(\theta_\mu h)^2 - V(h) + \frac{v^2}{4}T_r(D_\mu\Sigma^\dagger D^\mu\Sigma)[1 + 2c_v\frac{h}{v} + c_{2v}\frac{h^2}{v^2} + ...] \\ -m_i\bar{\psi}_{Li}\Sigma(1 + c_\psi\frac{h}{v} + ...)\psi_{Ri} + h.c.,\end{aligned} \tag{1}$$

Assuming that the couplings of the Higgs boson to SM fermions scale with their masses and do not violate flavor, the resulting effective Lagrangian can be parametrized as in equation 1, where $V(h)$ denotes the Higgs potential. The parameters cv, c_2v and $c\psi$ in 1, are in general arbitrary coefficients, normalised so that they equal 1 in the SM. The cv, c_2v and $c3$, which is not shown here, control the strength of the $hVV, hhVV$ and hhh couplings, respectively. A precision model-independent determination of c_2v would provide stringent constraints on a number of BSM scenarios. For generic values of cv and c_2v , the amplitude of the partonic scattering $VV->hh$ grows with the energy $\sqrt{s}$ until the contribution from the new states at the cut off scale Λ unitarizes it. The leading contribution in the energy range $m_W << \sqrt{s} << \Lambda$ comes from the scattering of longitudinal vector bosons and is given by:

$$\Lambda(V_LV_L->hh) \simeq s/v^2(c_2v - c^2v)$$

If the Higgs boson belongs to an electroweak doublet, as suggested by the LHC data, and the modifications to its couplings are small, then the values of c_2v and c^2v are in general predicted to be correlated [35][36] because there is a single dimension-6 effective operator (OH in the basis of [36])which controls the shift in both couplings. Therefore, a high-precision measurement of c_2v can test whether the Higgs boson belongs to a doublet in case a deviation is observed in cv [35].

The main analyses channels are $b\bar{b}\gamma\gamma$, $b\bar{b}\tau^+\tau^-$, and $b\bar{b}b\bar{b}$ where tha last channel full takes advantage of the high bb branching ratio [15][17][37]. Then $b\bar{b}\gamma\gamma$ has excellent trigger and mass resolution for photons. However $b\bar{b}\tau^+\tau^-$ final state is chosen in our case for the following reasons: first, taus are relatively clean, with small background; then, the branching ratio is relatively high and the b-jet tagging is very efficient thanks to the precise reconstruction of

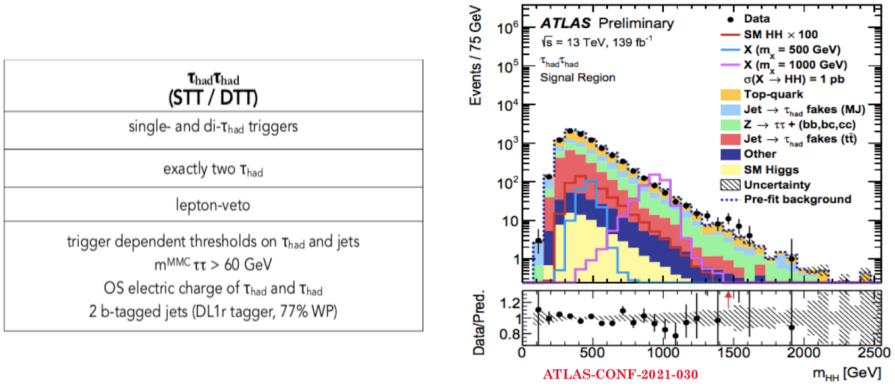

Figure 5. Event selection and backgrounds of $\tau_{had}\tau_{had}$ final state

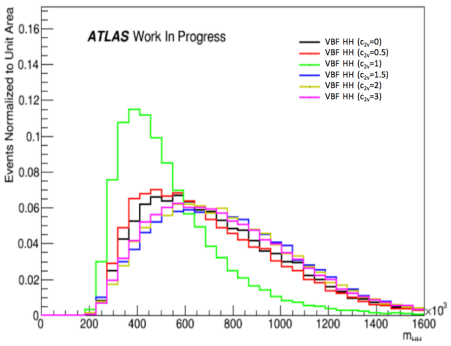

Figure 6. Gaining sensitivity to c_2v is achieved by reconstructing events with large values of m_{HH}

primary and secondary vertices; finally, despite the fact that tau lepton reconstruction might be quite challenging, efficient algorithms have been developed. This enhanced sensitivity to the underlying strength of the Higgs interactions makes double Higgs production via VBF a key process to test the nature of the electroweak symmetry breaking dynamics and to constrain the $hhVV$ quartic coupling. In this work, we revisit the feasibility of VBF Higgs pair production at the LHC and focus on the $HH- > b\bar{b}\tau^+\tau^-$ final state.

2.1. VBF jet Event Selection.
The analysis looks for jets with $p_T > 20GeV$ and $|\eta| < 2.5$ which are consistent with the same primary vertex and specifically looks for two tau-jets with the invariance mass of the di-τ system to be $> 60GeV$ and at least one b-jet with $p_T > 45GeV$. The tau-jets are jets with 1 or 3 tracks which are relatively isolated from activity around them, as expected by the fact that taus decay weakly, and b) two b-jets with energies $> 160GeV$, b-jets are jets which are 'b-tagged' because they contain tracks with a significant impact parameter with respect to the beam line, a requirement exploiting the long lifetime of b-quarks. In the VBF analyses we look for two additional jets consistent with the 'forward-backward' VBF topology (see Fig.4). These VBF jets are selected as follows:

- Baseline: Require 2 VBF jets in the event
- Take all forward jets ($|\eta| > 2.5$) with $p_T > 30GeV$.

- Take central jets only ($|\eta| < 2.5$, $p_T > 20GeV$) if they are non-btagged
- Find jet pairing with highest m_{jj} pair and in opposite hemispheres, ($\eta^{j1} * \eta^{j2} < 0$)
- Order VBF jets by p_T

The event selection for the $\tau_{had}\tau_{had}$ final state is shown in Fig.5, together with the event yields expected from the various sources for an integrated luminosity of $139fb^{-1}$ collected by ATLAS at $\sqrt{s} = 13TeV$. The way the di-Higgs mass (m_{HH}) distribution changes as the the c_2v value changes from it SM value ($c_2v = 1$) is shown in Fig.6.

Table 1.

Events	Total	VBF Selection
`VBF c2v=0`	6.77	4.54
`VBF c2v=1`	0.167	0.119
`VBF c2v=2`	4.63	3.125
`ggf`	5.40	1.57
`Comb.bkg`	3256.9	

3. Neural Network Design, Hyperparameter Optimization and Results

3.1. The Neural Network design and Input Variables

After comparison of various classification strategies, a Feed Forward Neural Network [38] was chosen in order to classify events in the VBF $bb\tau\tau$ topology. The even-numbered events in the Monte Carlo simulation samples are used to train the Network, which is built with the following characteristics:

- **Classification Strategy**
  - 3-class classification
  - VBF ($c_{2V} = 0$, $c_{2V} = 0.5$, $c_{2V} = 1.5$, $c_{2V} = 2$ - normalized) / ggF / Background
  - Training with even events
- **MultiLayer Perceptron**
  - Input Layer : 9 Neurons (relu)
  - Hidden Layers : $10 * 35$ Neurons (relu)
  - Output Layer : 3 Neuron (softmax)
  - Loss Function : Categorical Crossentropy
  - L2 Regularization for each hidden layer : $3 * 10^{-8}$
  - Loss Optimizer : ADAM
  - Batch size : 16
  - Epochs : 78

3.2. Input variables

- m_{HH} : Di-Higgs invariant mass
- $\Delta R_{\tau\tau}$: The ΔR between the visible-τ decay products
- ΔR_{bb} : The ΔR between the two b-jets

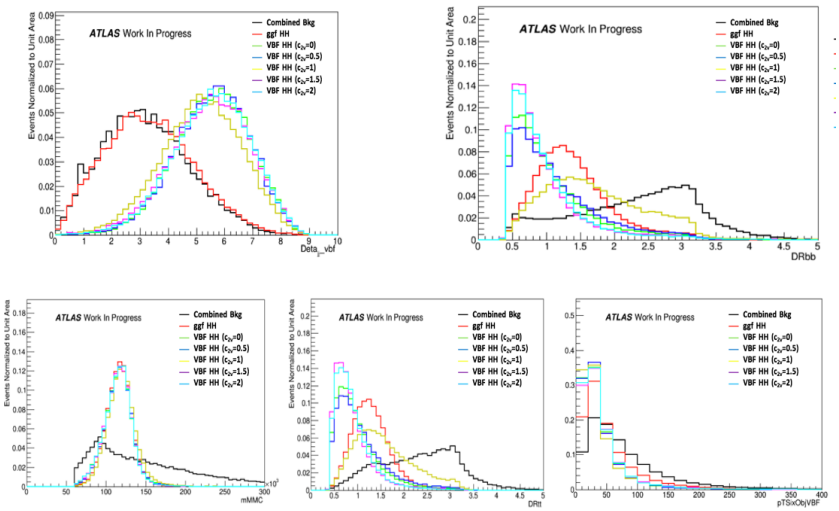

Figure 7. $\Delta\eta_{jj}$, ΔR_{bb}, m_{mmc}, $\Delta R_{\tau\tau}$, $p_T SixObj$ of VBF jets input variables of the NN

- $m_{\tau\tau}^{mmc}$: The invariant mass of the di-τ system, calculated using the MMC momenta of 2 taus [39]
- m_{bb} : The invariant mass of the di-b-jet system
- p_T^{jj} : Di-jet (VBF) transverse momentum
- m_{jj} : The invariant mass of the di-jet(VBF) system
- $\Delta\eta_{jj}$: The $\Delta\eta$ between the two VBF jets
- $\eta_{j1} * \eta_{j2}$: Product of η for two VBF jets
- Δphi_{jj} : The Δphi between the two VBF jets
- $p_T^{\tau\tau}$: The transverse momentum of the two taus
- p_T^{bb} : The transverse momentum of the two bs
- $p_T SixObj$: The transverse momentum of the HH+2-VBF jets

Some of these input variables are shown In Fig7, for background events, ggF HH events, as well as VBF HH events for various combinations of coupling values.

3.3. HyperParameter Optimisation

For the Hyperparameter Optimisation we used a Tree Parzen Estimator with Bayesian approach [40]. The Evaluations of a function are used to predict the next set of good hyperparameters The strategy is summarized in Table.2 and it allows a better overall performance and less time required for optimisation than random search. The Hyperparameters to optimise were:

- Neurons/layer : $20 - 40$
- Layers : $6 - 20$
- R2 value: $10^9 - 4 * 10^{-7}$
- Batch size: $4 - 24$

Different sets were used to perform 50 hyperparameter tests. The optimization variable was the signal for 5 background events.

Table 2. Hyperparameter Optimisation

Hyperparameter	Optimisation strategy	Implementation
Number of hidden layers	Bayesian optimization	TPE
Number of nodes in each layer	Bayesian optimization	TPE
Activation function	Typical suggestion for FF NN	ReLU
Output activation function	Typical suggestion for multiclassification NN	Softmax
Loss function	Typical suggestion for multiclassification NN	Cat. CrossEntropy
Loss minimizer	Dynamic adjustment of per-parameter learning rate	ADAM
Regularisation method	L2 typically works better than L1/Dropout	L2
Regularisation value	Bayesian optimization + fine tuning by hand	TPE
Batch size	Bayesian optimization	TPE
Epochs of training	Best validation loss	EarlyStopping

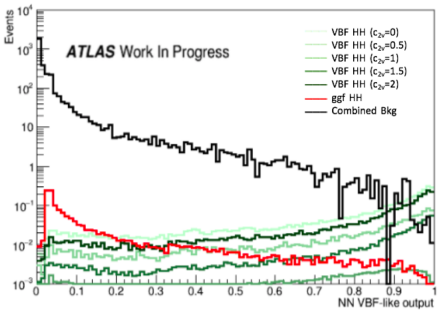

Figure 8. Comparison of various c_2v values of the VBF like ouput, compared with ggf and Combined Background

3.4. Results

The output of the NN described in this section is shown in Fig.8 for Background, ggF HH and VBF HH events, for various values of the c_2v coupling. The number of signal VBF HH, ggF HH and background event expected are shown in Table.1. Imposing a requirement on the minimum NN-output value, changes the remaining event yields and the signal significance is estimated as a function of the minimum NN-output value requirement (see Fig.10). The signal significance is calculated by [41] :

$$Sig = \sqrt{2((s+b)ln(1+s/b)-s)}$$

where s is the signal event yield and b is the sum of the ggF HH and background yields.

Overtraining tests were performed. The two Neural Networks were trained with the optimal Hyperparameters, one trained with the even and the other with the Odd events. Comparison of events is depicted in 10. In order to check that no overtraining is done with this network, two Neural Networks were trained with the optimal Hyperparameters; one trained with the even-numbered and the other with the odd-numbered events and the responses on the even and the odd sample of events were compared (see Fig. 10). Since no overtraining was observed, the results are presented. In order to perform the fit, which will be performed later in our analyses, a the transform tool (https://gitlab.cern.ch/CxAODFramework/TransformTool) will be used. The histograms will be re-binned using an automatic re-binning of the input histograms, which

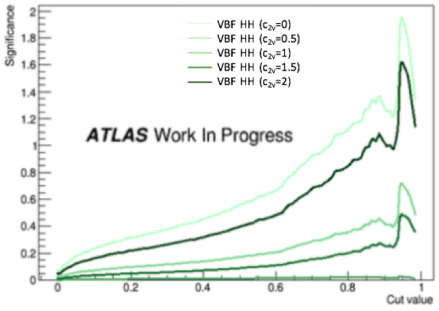

Figure 9. Values of the significance for the different samples Significance is calculated by

merges the histogram bins from right to left until some "pass" criteria are satisfied. In the $\tau_{had}\tau_{had}$ channel of the di-Higgs analysis the histograms are built with 1000 bins. The two chosen functions that will be used are giving better results for the fit performing better not only because they are allowing zero events in the last bin (which is not acceptable as it would cause fit instabilities and would not allow the usage of the asymptotic formula for the limit calculation) so they have been modified adding the requirement of the minimum 5 background events in bin.The fit function chosen as the rebinning function for this channel gives the optimal compromise between good sensitivity and number of bins and events per bin for fit stability. In the case of 5 background events, the NN-output cut which maximizes the signal significance is shown in Table.3, together with the expected signal yield and significance. The expected signal significance is improved considerably, compared to our standard analyses.

Table 3. Significance meausurements

c2v	Significance	Cut value for 5 bkg events	Signal events passing cut	Bkg events passing cut
0	1.082	0.78	2.820 ± 0.022	5.06 ± 0.784
0.5	0.343	0.78	0.842 ± 0.008	5.06 ± 0.784
1	0.019	0.78	0.045 ± 0.004	5.06 ± 0.784
1.5	0.190	0.78	0.0460 ± 0.003	5.06 ± 0.784
2	0.814	0.78	2.076 ± 0.017	5.06 ± 0.784

4. Concusion

This contribution presented studies about accessing the SM Higgs couplings and BSM physics with di-higgs (HH) VBF events in the $bb\tau\tau$ final state. A Feed Forward NN design was chosen to separate the VBF HH signal from ggF HH and background events. A set of good Hyperparameters were found for the NN architecture and additional tests were performed to check if there is overtraining. The signal significance was studied for various c_2v coupling values, with c_2v=1 being the SM value. Since the NN demonstrated a significant improvement in the signal significance, this NN is implemented in our Analysis framework

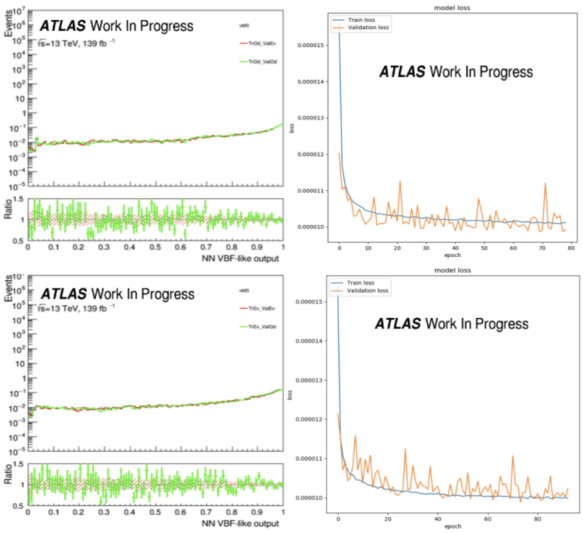

Figure 10. Overtraining tests of the NN. Training was performed with different sets of Even and Odd events

5. Acknowledgments

We acknowledge support of this work by the project "DeTAnet: Detector Development and Technologies for High Energy Physics" (MIS 5029538) which is implemented under the action "Reinforcement of the Research and Innovation Infrastructure" funded by the Operational Programme "Competitiveness, Entrepreneurship and Innovation" (NSRF 2014-2022) and co-financed by Greece and the European Union (European Regional Development Fund).

References

[1] G. Aad, et al., Phys. Lett. B716, 1 (2012). DOI 10.1016/j.physletb.2012.08.020
[2] S. Chatrchyan, et al., Phys. Lett. B716, 30 (2012). DOI 10.1016/j.physletb.2012.08.021
[3] A. Belyaev, M. Drees, O.J.P. Eboli, J.K. Mizukoshi, S.F. Novaes, in Proceedings, International Europhysics Conference on High energy physics (EPS-HEP 1999): Tampere, Finland, July 15-21, 1999 (1999), pp. 748?751. URL http://alice.cern.ch/format/showfull? sysnb=0330978
[4] B. Grinstein, M. Trott, Phys. Rev. D76, 073002 (2007). DOI 10.1103/PhysRevD.76.073002
[5] R. Grober, M. Muhlleitner, JHEP 06, 020 (2011). DOI 10.1007/JHEP06(2011)020
[6] J. Cao, Z. Heng, L. Shang, P. Wan, J.M. Yang, JHEP 04, 134 (2013). DOI 10.1007/JHEP04(2013)134
[7] D. de Florian, et al., Handbook of LHC Higgs Cross Sections: 4. Deciphering the Nature of the Higgs Sector. Tech. rep. (2016)
[8] M. Grazzini et al., Higgs boson pair production at NNLO with top quark mass effects, JHEP 05 (2018) 059, arXiv: 1803.02463 [hep-ph]
[9] R. Contino, C. Grojean, M. Moretti, F. Piccinini, R. Rattazzi, JHEP 05, 089 (2010). DOI 10.1007/JHEP05(2010)089
[10] M. Gouzevitch, A. Oliveira, J. Rojo, R. Rosenfeld, G.P. Salam, V. Sanz, JHEP 07, 148 (2013). DOI 10.1007/JHEP07(2013)148
[11] R. Barbieri, D. Buttazzo, K. Kannike, F. Sala, A. Tesi, Phys. Rev. D87(11), 115018 (2013). DOI 10.1103/PhysRevD.87.115018
[12] U. Ellwanger, JHEP 08, 077 (2013). DOI 10.1007/JHEP08(2013)077
[13] M. Moreno Llacer et al., Study of the CP properties of the top-quark Yukawa interaction in $\tau\bar{\tau}H$ and τH events with $H->\gamma\gamma$, tech. rep. ATL-COM-PHYS-2019-961, CERN, 2019, url: https://cds.cern.ch/record/2684286
[14] G. Branco et al., Theory and phenomenology of two-Higgs-doublet models, Phys. Rept. 516 (2012) 1, arXiv: 1106.0034 [hep-ph]
[15] ATLAS Collaboration, Searches for Higgs boson pair production in the $hh->bb\tau\tau, \gamma\gamma WW, \gamma\gamma bb, bbbb$

channels with the ATLAS detector, Phys. Rev. D 92 (2015) 092004, doi:10.1103/PhysRevD.92.092004, arXiv:1509.04670.
[16] ATLAS Collaboration, Search for Higgs boson pair production in the $bbWW$ decay mode at $\sqrt{s} = 13TeV$ with the ATLAS detector, JHEP 04 (2019) 092, arXiv: 1811.04671 [hep-ex]
[17] ATLAS Collaboration, Search for pair production of Higgs bosons in the $b\bar{b}b\bar{b}$ final state using proton-proton collisions at $\sqrt{s} = 13TeV$ with the ATLAS detector, JHEP 01 (2019) 030, arXiv: 1804.06174 [hep-ex]
[18] A.?M. Sirunyan et al. (CMS Collaboration), Search for Higgs boson pair production in the $bb\tau\tau$ final state in proton-proton collisions at $\sqrt{s} = 8TeV$, Phys. Rev. D 96, 072004
[19] D. de Florian, C. Grojean, F. Maltoni, C. Mariotti, A. Nikitenko, M. Pieri, P. Savard, M. Schumacher, R. Tanaka, Handbook of LHC Higgs cross sections: 4. Deciphering the nature of the Higgs sector, CERN-2017-002-M, DOI: https://doi.org/10.23731/CYRM-2017-002
[20] M.J. Dolan, C. Englert, M. Spannowsky, JHEP 10, 112 (2012). DOI 10.1007/JHEP10(2012)112
[21] A. Papaefstathiou, L.L. Yang, J. Zurita, Phys. Rev. D87(1), 011301 (2013). DOI 10.1103/PhysRevD.87.011301
[22] A.J. Barr, M.J. Dolan, C. Englert, M. Spannowsky, Phys. Lett. B728, 308 (2014). DOI 10.1016/j.physletb.2013.12.011
[23] B. Cooper, N. Konstantinidis, L. Lambourne, D. Wardrope, Phys. Rev. D88(11), 114005 (2013). DOI 10.1103/PhysRevD.88.114005
[24] C.T. Lu, J. Chang, K. Cheung, J.S. Lee, JHEP 08, 133 (2015). DOI 10.1007/JHEP08(2015)133
[25] D. Wardrope, E. Jansen, N. Konstantinidis, B. Cooper, R. Falla, N. Norjoharuddeen, Eur. Phys. J. C75(5), 219 (2015). DOI 10.1140/epjc/ s10052-015-3439-0
[26] S. Dawson, S. Dittmaier, M. Spira, Phys. Rev. D58, 115012 (1998). DOI 10.1103/PhysRevD.58.115012
[27] D. de Florian, J. Mazzitelli, Phys. Rev. Lett. 111, 201801 (2013). DOI 10.1103/PhysRevLett.111.201801
[28] D.Y. Shao, C.S. Li, H.T. Li, J. Wang, JHEP 07, 169 (2013). DOI 10.1007/JHEP07(2013)169
[29] D. de Florian, J. Mazzitelli, JHEP 09, 053 (2015). DOI 10.1007/JHEP09(2015)053
[30] G.F. Giudice, C. Grojean, A. Pomarol, R. Rattazzi, JHEP 06, 045 (2007). DOI 10.1088/1126-6708/2007/06/045
[31] L.S. Ling, R.Y. Zhang, W.G. Ma, L. Guo, W.H. Li, X.Z. Li, Phys. Rev. D89(7), 073001 (2014). DOI 10.1103/PhysRevD.89.073001
[32] M.J. Dolan, C. Englert, N. Greiner, K. Nordstrom, M. Spannowsky, Eur. Phys. J. C75(8), 387 (2015). DOI 10.1140/epjc/s10052-015-3622-3
[33] J. Baglio, A. Djouadi, R. Grber, M.M. Mhlleitner, J. Quevillon, M. Spira, JHEP 04, 151 (2013). DOI 10.1007/JHEP04(2013)151
[34] D.B. Kaplan, H. Georgi, Phys. Lett. B136, 183 (1984). DOI 10.1016/0370-2693(84)91177-8
[35] R. Contino, C. Grojean, D. Pappadopulo, R. Rattazzi, A. Thamm, JHEP 02, 006 (2014). DOI 10.1007/JHEP02(2014)006
[36] G.F. Giudice, C. Grojean, A. Pomarol, R. Rattazzi, JHEP 06, 045 (2007). DOI 10.1088/1126-6708/2007/06/045
[37] ATLAS Collaboration, Search for Higgs boson pair production in the $\gamma\gamma b\bar{b}$ final state with $\sqrt{s} = 13TeV$ collision data collected by the ATLAS experiment, JHEP 11 (2018) 040, arXiv: 1807.04873 [hep-ex]
[38] Daniel Svozil, Vladimr Kvasnicka, Ji Pospichal,Introduction to multi-layer feed-forward neural networks,Chemometrics and Intelligent Laboratory Systems, Volume 39, Issue 1,1997,Pages 43-62,ISSN 0169-7439,https://doi.org/10.1016/S0169-7439(97)00061-0.
[39] A. Elagin, P. Murat and A. Safanov, 'A New Mass Reconstruction Technique for Resonances Decaying to $\tau\tau$', arXiv:1012.4686v2 [hep-ex] 22-Feb-2011
[40] Yoshihiko Ozaki, Yuki Tanigaki, Shuhei Watanabe, Masaki Onishi, Multiobjective tree-structured parzen estimator for computationally expensive optimization problems, GECCO '20: Proceedings of the 2020 Genetic and Evolutionary Computation Conference, June 2020, Pages 533?541, https://doi.org/10.1145/3377930.3389817
[41] Glen Cowan, Kyle Cranmer, Eilam Gross, Ofer Vitells, Asymptotic formulae for likelihood-based tests of new physics, Eur. Phys. J. C (2011) 71: 1554 DOI 10.1140/epjc/s10052-011-1554-0